XVIII IMEKO WORLD CONGRESS
Metrology for a Sustainable Development
September, 17 – 22, 2006, Rio de Janeiro, Brazil

FAST INTEGRAL OPTICAL ROUGHNESS MEASUREMENT OF SPECULAR REFLECTING SURFACES IN THE NANOMETER RANGE

S. Patzelt, F. Horn, G. Goch

University of Bremen - FB 4 - Faculty of Production Engineering - Department of Measurement and Control - Badgasteiner Straße 1
28359 Bremen – Germany, patzelt@msr.uni-bremen.de, F.Horn@msr.uni-bremen.de, gg@biba.uni-bremen.de

Abstract: A fast optical roughness measuring device with a compact design is presented. The measuring principle is based on double scattering of coherent light. The measurement results in an integral statistical roughness value like Ra or Rq according to ISO 4287. It is valid for the illuminated surface area with diameters between 0.5 mm and 10 mm at a resolution of about 1 nm (Ra-value). A simulation model of the optical roughness measuring process based on the Huygens-Fresnel approximation was implemented. The simulation tool enables to investigate potential improvements of the measuring method without expensive and time consuming experiments.

Keywords: Roughness, doubly scattered laser light, speckle correlation, simulation.

1. INTRODUCTION

Industrial production processes for optically smooth surfaces (Ra < $\lambda/8$, [1]) show an increasing demand for monitoring the surface quality, while the workpiece is still clamped inside the machine tool (in-situ) or even during machining (in-process). An appropriate roughness measuring device should operate fast and non-contacting with a working distance of at least some centimeters. Measurements of both opaque and transparent materials should be possible.

In this context, many investigations concerning the statistical properties of speckle patterns produced by coherent illumination have been carried out [2–6]. It was found that speckle patterns provide information about surface roughness. Therefore, speckle techniques have a high potential for surface inspection applications. In connection with modern electro-optical devices (e.g. high power laser diodes, CMOS and CCD cameras), speckle methods show real-time and in-process capabilities [7–10].

This paper deals with the roughness measuring method based on doubly scattered coherent light as described in [11]. The method enables to determine surface roughness in a range of Ra = 1 nm to Ra = 100 nm, with the arithmetic mean roughness Ra according to DIN ISO 4287. The theoretical background is based on the statistical properties of speckle patterns that are generated in the Fresnel region, when a rough surface is illuminated with a fully developed static speckle pattern. Former studies on this subject concern speckle patterns from deep random phase screens, i.e., transmitting surfaces with isotropic height fluctuations [12-14]. A more general theoretical description of static speckle patterns scattered from diffuse or reflecting rough surfaces can be found in [15]. It is valid for both isotropic and anisotropic roughness, which are typically produced by mechanical processes such as grinding.

Fig. 1 shows the conventional double scattering measuring set-up for roughness characterization.

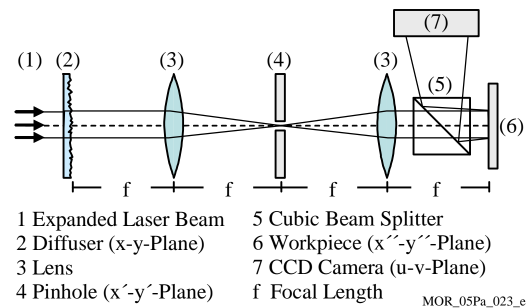

Fig. 1. Double scattering roughness measuring set-up.

A diffuser glass (2) scatters an expanded laser beam (1) and generates a speckle pattern. A 4-f lens arrangement with a pinhole (4) in the common focus between the lenses (3) acts as a low-pass filter and forms an illumination speckle pattern with a well defined diameter and a well defined mean speckle size. According to the Huygens principle, this light intensity distribution is the result of the superposition of infinite secondary wavelets that emerge from the diffuser plate. In the workpiece plane (6), the phase distribution of all secondary wavelets is very sensitive to additional optical path differences. Hence, even optically smooth workpiece topographies influence the phase distribution of the incident speckle pattern and modulate the single speckle intensities. Therefore, the CCD camera (7) detects a specularly reflected and scattered speckle pattern, which shows a roughness dependent intensity modulation (Fig. 7).

So far, the corresponding measuring set-up is too large for a machine integration. Furthermore, a sufficient roughness resolution is obtained only, if the diameter of the illumination pattern exceeds 1 mm, at least. Especially for the production of complex optical elements (lenses, mirrors, replication tools and molds), a strong demand exists for smaller measuring areas (e.g. for microstructured surfaces)

and for a better resolution of surface heights in the nanometer range.

The following describes the further development of the roughness measuring technique based on double scattering. The measuring process was completely modeled based on the scalar Kirchhoff diffraction theory. As a result of the simulations, some components of the measuring device were changed in order to improve the performance (i.e., resolution and size of set-up). For example, a shorter visible wavelength (λ = 405 nm) promises a better resolution of surface details than the red or infrared laser light (λ = 650 nm, λ =810 nm) used so far. Fortunately, prices and emitted light wavelengths of laser diodes decrease, while at the same time the output power and life times increase. Thus, blue emitting laser diodes become very attractive for measuring purposes. Another improvement resulted from the experimental investigations: An optical multimode fiber replaces the diffuser glass as well as the 4-f spatial filter and generates the illumination speckle pattern with a well defined mean speckles size. The fiber optical measuring set-up is much more compact than the former one with free beam propagation.

Since the roughness measuring method of double scattering is based on statistical optics, the parameters that are used for roughness characterization should be of statistical importance. Hence, the surface description is based upon the rms-deviation Rq and the arithmetical mean deviation Ra as surface amplitude parameters:

$$\mathrm{Rq} = \sqrt{\frac{1}{l_r}\int_0^{l_r} h^2(x)\,dx}\,; \quad \mathrm{Ra} = \frac{1}{l_r}\int_0^{l_r} |h(x)|\,dx, \qquad (1)$$

with the sampling length l_r. For a Gaussian height distribution $h(x)$ the relation $\mathrm{Rq} = \sqrt{\pi/2}\cdot\mathrm{Ra}$ is valid. Two-dimensional measuring methods often refer to the surface rms-deviation Sq and the surface arithmetic mean roughness Sa, which are the two-dimensional analogues of the roughness profile parameters Rq and Ra. Up to now, Sa and Sq are not standardized. In statistical optics, the lateral structure of the surface is generally characterized by the normalized surface autocorrelation function $\rho_h(x)$:

$$\rho_h(x) = \frac{\int_0^L h(\xi)h(x+\xi)d\xi}{\int_0^L h^2(\xi)d\xi}\,; \quad \rho_h(\Lambda_k) = 1/e\,, \qquad (2)$$

which leads to the surface correlation length Λ_k.

2. SIMULATION OF THE MEASURING PROCESS

A reasonable simulation of the measuring process should cover both the generation of an isotropically rough model surface and the calculation of the doubly scattered light intensities in the observation plane. The wave optical simulation model is based on the scalar diffraction theory with respect to the Kirchhoff boundary conditions [16]. All algorithms are implemented in *Matlab*.

2.1. *Generation of model surfaces*

The numerical surface generation algorithm is a two-dimensional expansion of the procedure proposed in [17]. A pseudo random number generator creates a two-dimensional array of normally distributed surface height values with zero mean. A Gaussian filter function smoothes the surface heights. The width of the filter function is the desired lateral surface correlation length Λ_k from Eq.(2). Finally, the height distribution is scaled to the appropriate rms-roughness. Fig. 2 shows examples of two isotropically rough surfaces with the same lateral correlation length $\Lambda_k = 8.8\ \mu\mathrm{m}$, but different roughness $\mathrm{Sq} = 10\ \mathrm{nm}$ and $\mathrm{Sq} = 50\ \mathrm{nm}$, respectively. Both surface models consist of 1000×1000 height values with a lateral distance $\Delta x = \Delta y = 1\ \mu\mathrm{m}$.

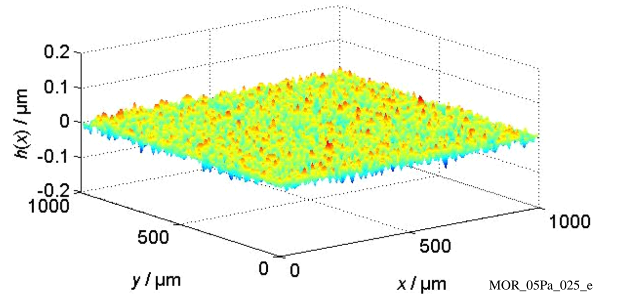

a)

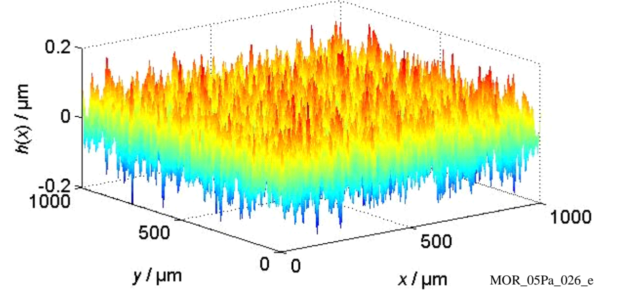

b)

Fig. 2. Modeled surfaces with the lateral correlation length $\Lambda_k = 8.8\ \mu\mathrm{m}$ and isotropic roughness: a) Sq = 10 nm, b) Sq = 50 nm.

2.2. *Simulation of the double light scattering process*

The light scattering simulation model describes the interactions of the coherent light with the optical components along its path through the diffuser glass and the 4-f spatial filter set-up, via the workpiece surface to the observation plane in the Fresnel region (Fig. 1). Assuming a plane wave of the incident expanded laser beam

$$E(x,y) = E_0(x,y)\cdot e^{ik\sqrt{x^2+y^2}}, \qquad (3)$$

the Gaussian beam intensity profile

$$E_0(x,y) = E_0 \cdot e^{\left(-\frac{x^2}{\sigma_x^2}-\frac{y^2}{\sigma_y^2}\right)} \qquad (4)$$

is characterized by the beam radius $\sigma_x = \sigma_y = 2.5$ mm, at which the intensity is decreased to $1/e^2$ of the maximum value in the beam center, i.e. the optical axis. The ground glass leads to a phase modulation $\phi_1(x,y)$ of the plane wave, which is related to the surface heights $h_d(x,y)$ of the diffuser

$$\phi_1(x,y) = k \cdot (n-1) \cdot h_d(x,y) \; , \tag{5}$$

with the refractive index n of the transparent medium and the wave number $k = 2\pi/\lambda$. Due to the special 4-f arrangement, both double convex lenses perform a Fourier transformation or an inverse Fourier transformation, respectively [16]. The phase and amplitude in the x'-y'-plane of the pinhole are related to the phase and amplitude in the diffuser plane by:

$$E_{s1}(x',y') = \int E_{s1}(x,y) \cdot e^{-i\frac{2\pi}{\lambda f}(x \cdot x' + y \cdot y')} dxdy \; . \tag{6}$$

The index $s1$ denominates the first light scattering process. The pinhole with a radius r_{PH} in the back focal plane of the first lens is modeled by a cylinder function:

$$cyl(x',y') = \begin{cases} 1 & \text{for} \quad \sqrt{x'^2 + y'^2} < r_{PH} \\ 0 & \text{else} \end{cases} \; . \tag{7}$$

The second lens performs an inverse Fourier transformation of the product of the electrical field in front of the pinhole according to Eq.(6) and the cylinder function according to Eq.(7). The result is the electrical field $E_{s1}(x'',y'')$ in the back focal plane of the second lens. Considering the ratio of the two focal lengths, the resulting field distribution directly in front of the object describes an illumination speckle pattern with both a well defined diameter and a well defined mean speckle size. The interaction of this biased wave front with the surface $h_w(x'',y'')$ of the reflecting workpiece topography leads to a second phase modulation $\phi_2(x'',y'')$ of the incident field

$$E_{s2}(x'',y'') = E_{s1}(x'',y'') \cdot e^{i\phi_2(x'',y'')} \; , \tag{8}$$

with

$$\phi_2(x'',y'') = -2k \cdot h_w(x'',y'') \cdot \cos\Theta_i \; . \tag{9}$$

Here, the angle of incidence is $\Theta_i = 90°$. The index $s2$ denotes the second light scattering process. Finally, the electrical field $E_{s2}(u,v)$ on the camera CCD-chip, located at a distance a from the workpiece (i.e. in the Fresnel region) follows from $E_{s2}(x'',y'')$ in connection with the Fresnel diffraction integral [16]:

$$E_{s2}(u,v) = \frac{-ike^{ika}}{2\pi a} \iint\limits_{S_0} E_{s2}(x'',y'') \cdot e^{\frac{ik}{2a}\left[(u-x'')^2 + (v-y'')^2\right]} \, \mathrm{d}x''\mathrm{d}y'' \; . \tag{10}$$

Eq.(10) represents a convolution integral. Therefore, according to the convolution theorem, it can easily be implemented by the use of fast Fourier transform algorithms in *Matlab*.

2.3. *Simulation results*

Fig. 3 shows calculated scattered intensity distributions for two different smooth objects as a result of the simulations described above. As readily can be seen, the illumination speckle pattern is the same in Fig. 3.a and 3.b. However, due to the rougher workpiece, the speckle intensities in Fig. 3.b appear modulated.

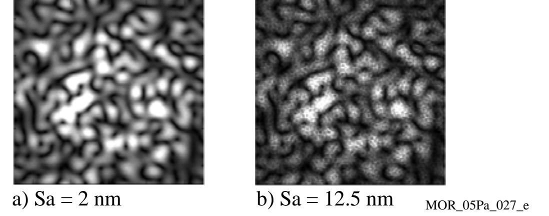

Fig. 3. Simulated doubly scattered speckle patterns from surfaces with isotropic roughness: a) Sq = 2 nm, b) Sq = 12,5 nm.

2.4. *Evaluation*

An appropriate optical roughness parameter Ropt should characterize the mean speckle size within a scattered light intensity distribution according to Fig. 3. The determination of such a parameter is based on the calculation of a two-dimensional discrete speckle intensity autocorrelation function (ACF). The ACF gradient near to the ACF maximum increases as the speckle intensities become more modulated (Fig. 4).

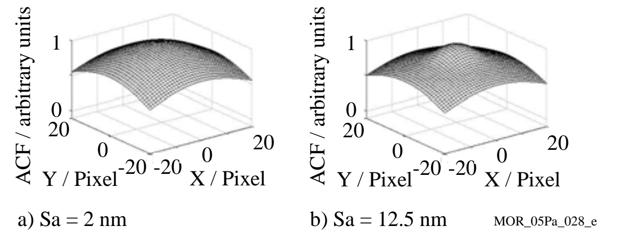

Fig. 4. Two-dimensional autocorrelation functions (ACF) of the simulated speckle intensity distributions in a) Fig. 3.a and b) Fig. 3.b.

Hence, flat slopes indicate smooth surfaces, while steeper slopes result from a larger roughness.

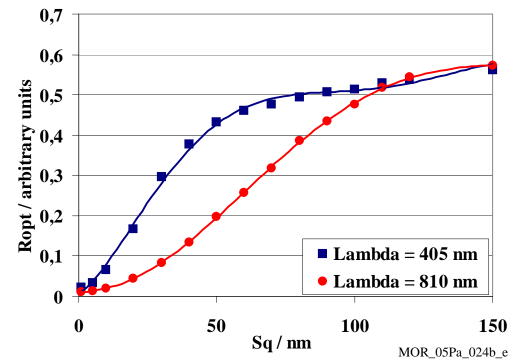

Fig. 5. Optical roughness parameter Ropt vs. rms-roughness Sq for simulated doubly scattered speckle patterns and two different laser wavelengths: λ = 405 nm (squares), λ = 810 nm (dots).

Fig. 5 presents the dependence of the optical parameter Ropt on the Sq-roughness of different isotropic rough model surfaces in the range between Sq = 1 nm and Sq = 150 nm. A sufficient correlation between both parameters exist for roughness values between Sq = 1 nm and Sq = 100 nm. Furthermore, the resolution of the measuring method can be enhanced for smooth surfaces by the use of light with a shorter wavelength.

3. EXPERIMENTAL ROUGHNESS CHARACTERIZATION

This section explains conceptual improvements of the measuring device.

3.1. Fiber optical measuring set-up

The collimated beam of a blue emitting laser diode ($\lambda = 405$ nm) is coupled into a multimode fiber (core diameter 50 µm, cladding diameter 125 µm, fiber length 1 m) by an high aperture laser objective (Fig. 6). Due to internal mode coupling the output fiber end emits a divergent speckled intensity field. An appropriate achromatic lens creates a slightly convergent beam that illuminates the workpiece surface. The surface (diffusely) reflects the intensity distribution via a beam splitter to a CCD camera (640 x 480 pixels, 8 bit intensity resolution).

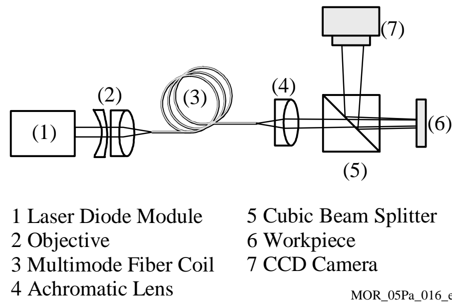

Fig. 6. Measuring set-up.

Lateral shifting and tilting of the fiber input end influences the mean speckle size as well as the spatial speckle distribution. This enables to generate a speckle pattern of well defined extension and speckle diameter on the investigated surface. Therefore, the fiber combines the two functions of speckle generation and spatial filtering. The fiber has to be well protected against mechanical stress and temperature changes in order to avoid sudden changes of the speckle intensity distribution. Depending on the focal length of the achromatic lens (4); the diameter of the illumination speckle pattern is $d > 0.5$ mm. Thus, measurements at microstructured surfaces, e.g. v-grooves, are possible in principle, if the angle between the flanks is 90°, at least.

3.2. Roughness measurements

Fig. 7 shows images of the same illumination speckle pattern after scattering at two different polished surfaces. While the smooth surface nearly specularly reflects the original pattern (Fig. 7.a), the rougher surface modulates the speckle intensities (Fig. 7.b). Due to the anisotropic manual polishing process (vertical direction in Fig. 7.b), the mean speckle diameter decreases mainly in the horizontal *x*-direction.

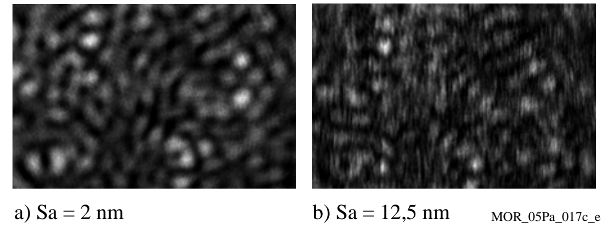

Fig. 7. Images of the same illumination speckle pattern scattered from surfaces of different roughness.

3.3. Evaluation

Fig. 8 presents two-dimensional discrete speckle intensity autocorrelation functions of the speckle patterns from Fig. 7.

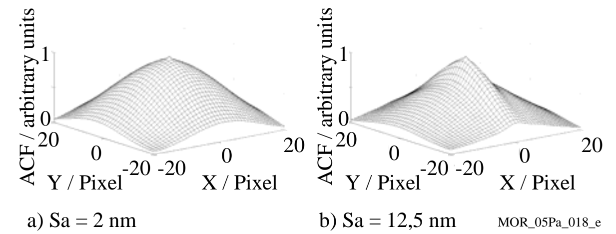

Fig. 8. Two-dimensional autocorrelation functions (ACF) of the speckle intensity distributions in a) Fig. 7.a and b) Fig. 7.b.

Although this measuring method gives an integral roughness value for the illuminated surface area, it is possible to distinguish the roughness in different directions, e.g. if the surface topography is anisotropic. Therefore, the ACF slope has to be determined separately for the *x*-, *y*- or any other direction of interest within the speckle image.

3.4. Results

Fig. 9 shows measuring results for six smooth surfaces of different roughness.

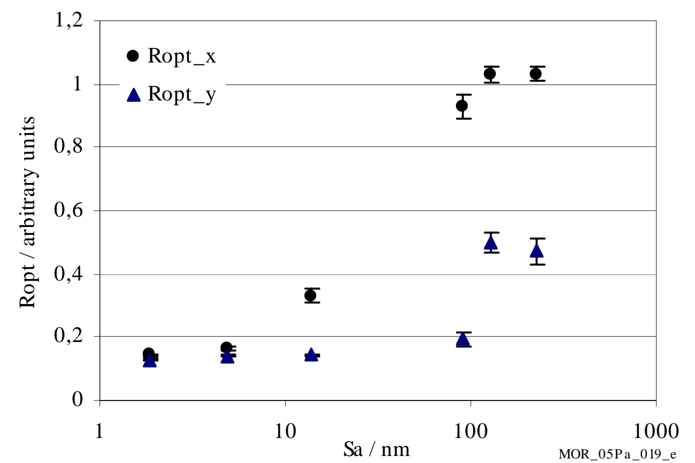

Fig. 9. Measuring results of the double scattering method compared to reference roughness values obtained with a white light interferometer.

The optical parameters Ropt_x and Ropt_y characterize the roughness in the *x*- and the *y*-direction on the surfaces. The roughness in *x*-direction always exceeds the roughness in *y*-direction, which is a result of the anisotropic polishing process. The error bars give the standard deviation for ten measurements at different areas of each surface. The values of the integral roughness parameter Sa were obtained by white light interferometer (WLI) measurements. Due to the very small error bars the measuring method enables to distinguish roughness differences of about $\Delta Sa = 1$ nm even for optically smooth surfaces with $Sa < 20$ nm. The measuring range of the double scattering measuring principle is limited to nearly specularly reflecting surfaces between Sa = 1 nm and Sa = 100 nm.

4. CONCLUSION

The simulation of measuring process in connection with experimental investigations lead to further improvements of the integral roughness measuring method based on double light scattering. The performance of the measuring device was enhanced by using a short light wavelength and a multimode fiber. The generated blue illumination speckle pattern is very sensitive to roughness variations of the inspected surfaces in the range below Sa = 50 nm. The small illumination spot diameter (> 0.5 mm) allows a high spatial resolution as well as roughness measurements of microstructured surfaces. The length of the fiber optical set-up only extends a few centimeters, which enables the measuring device to be integrated into machine tools and to perform in-situ or in-process measurements. A first approach for an in-process application aims at ultra precise milling techniques for the generation of complex optical mold inserts. Furthermore, process accompanying optical measurements are conceivable in connection with subsequent polishing of high precision molds for the replication of structured optical elements, which are generated by diamond machining or precision grinding.

ACKNOWLEDGMENTS

The authors gratefully acknowledge the funding by the Transregional Cooperative Research Center (SFB/TR4) [18], given by the Deutsche Forschungsgemeinschaft (DFG).

REFERENCES

[1] J.A. Ogilvy, "Theory of Wave Scattering from Random Rough Surfaces", Bristol, Hilger, 1991.

[2] G. Parry, "Speckle patterns in partially coherent light", in Dainty J. C.: Laser Speckle and Related Phenomena, Topics in Applied Physics Series, Vol. 9, Berlin, Springer-Verlag, 1975.

[3] H.M. Pedersen, "Second-order statistics of light diffracted from gaussian, rough surfaces with applications to the roughness dependence of speckles", Opt. Act., Vol. 22, No. 6, pp. 523-535, 1975.

[4] G.R.C. Reddy, V.V. Rao, "Correlation of speckle patterns generated by a diffuser illuminated by partially coherent light", Opt. Acta, No. 30, pp. 1213–1216, 1983.

[5] K.A. O'Donnell, "Speckle statistics of doubly scattered light", J. Opt. Soc. Am., No. 72, pp. 1459–1463, 1982.

[6] R. Barakat, "Second- and fourth-order statistics of doubly scattered speckle", Opt. Acta, No. 33, pp. 79–89, 1986.

[7] M. Giglio, S. Musazzi, U. Perini, "Surface roughness measurements by means of speckle wavelength decorrelation", Opt. Commun., Vol. 28, No. 2, pp. 166-170, 1979.

[8] T.V. Vorburger, E.C. Teague, "Optical techniques for on-line measurement of surface topography", Prec. Eng., Vol. 3, pp. 61-83, 1981.

[9] P. Lehmann, S. Patzelt, A. Schöne, "Surface Roughness Measurement by Means of Polychromatic Speckle Elongation", Appl.Opt., Vol. 36, No. 10, pp. 2188-2197, 1997.

[10] P. Lehmann, G. Goch, "Comparison of conventional light scattering and speckle techniques concerning an in-process characterization of engineered surfaces", Ann. of the CIRP, Vol. 49/1, pp. 419-422, 2000.

[11] S. Patzelt, G. Goch, "Scattered light techniques for surface characterization of optical components", XI. Internationales Oberflächenkolloquium, Chemnitz, Shaker Verlag, Aachen, pp. 214-223, 2004.

[12] K. Nakagawa, T. Yoshimura, T. Minemoto, "Surface-roughness measurement using Fourier transformation of doubly scattered speckle pattern", Appl. Opt., Vol. 32, pp. 4898-4903, 1993.

[13] T. Yoshimura, K. Kazuo, K. Nakagawa, "Surface roughness dependence of the intensity correlation function under speckle pattern illumination", J. Opt. Soc. Am., Vol. A 7, pp. 2254-2259, 1990.

[14] L. Basano, S. Leporatti, P. Ottonello, V. Palestini, R. Rolandi, "Measurements of surface roughness: use of a CCD camera to correlate doubly scattered speckle patterns", Appl. Opt., Vol. 34, pp. 7286-7290, 1995.

[15] P. Lehmann, "Surface roughness measurement based on the intensity correlation function of scattered light under speckle-pattern illumination", Appl. Opt., Vol. 38, No. 7, pp. 1144-1152, 1999.

[16] J.W. Goodman, "Introduction to Fourier Optics", New York, McGraw-Hill, 1996.

[17] P. Lehmann, A. Schöne, J. Peters, "Simulation der Lichtstreuung an technischen rauhen Oberflächen als Grundlage laseroptischer Rauheitsmessverfahren", Forschung im Ingenieurwesen - Engineering Research, Vol. 59, VDI, 1993.

[18] Transregional Cooperative Research Center (SFB/TR4), http://www.sfb-tr4.uni-bremen.de, 2006.